

## FIGURES

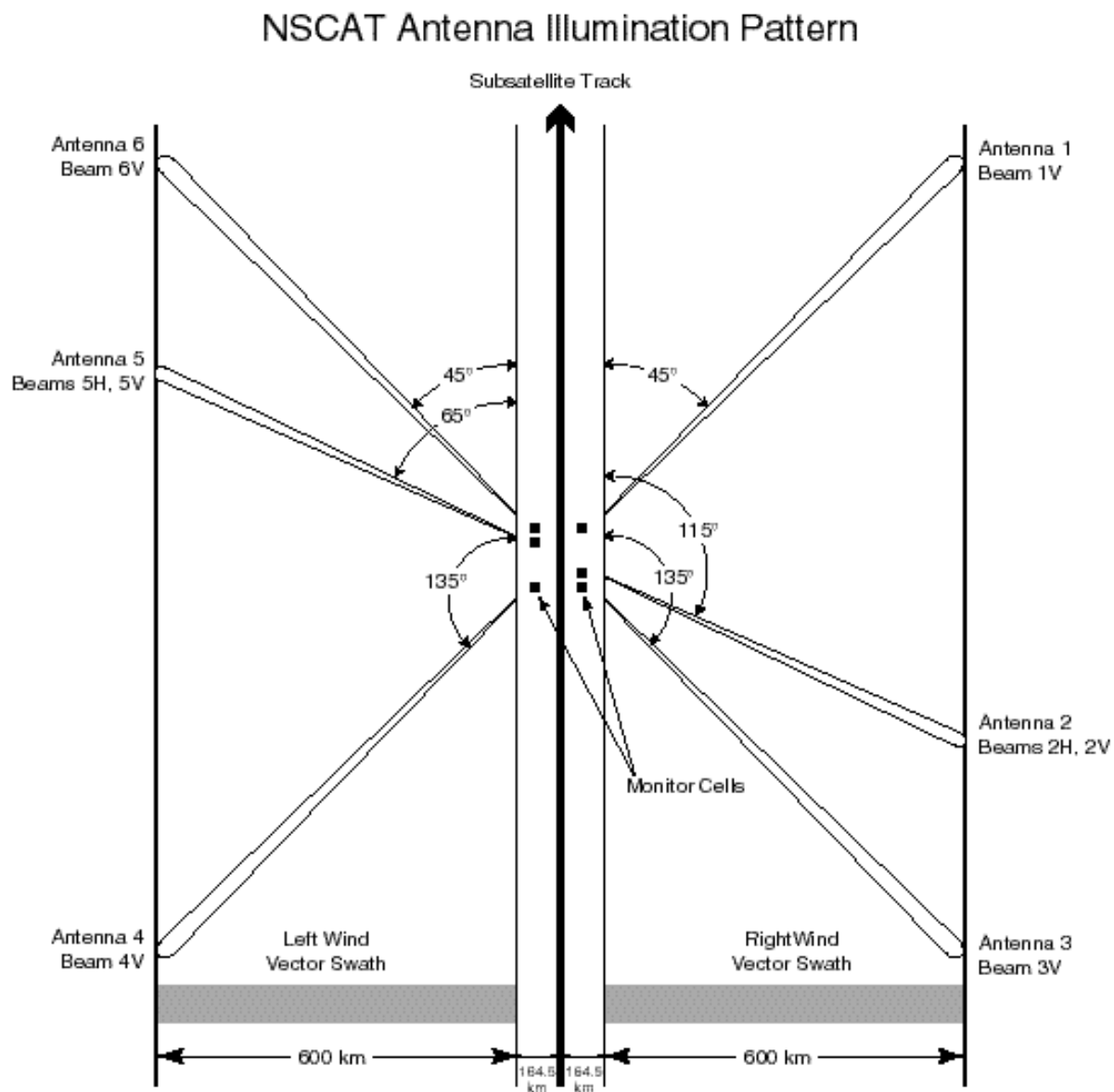


Fig. 1 : NSCAT antenna illumination pattern and the two swaths.

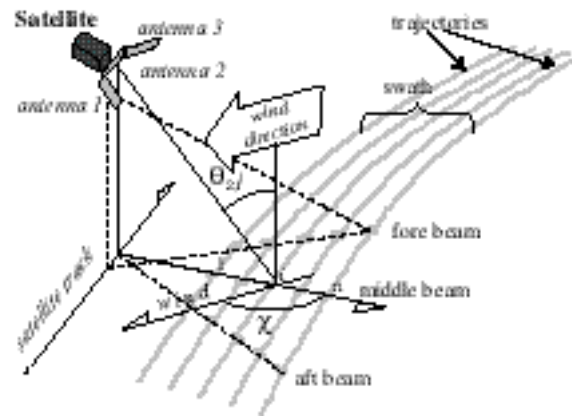
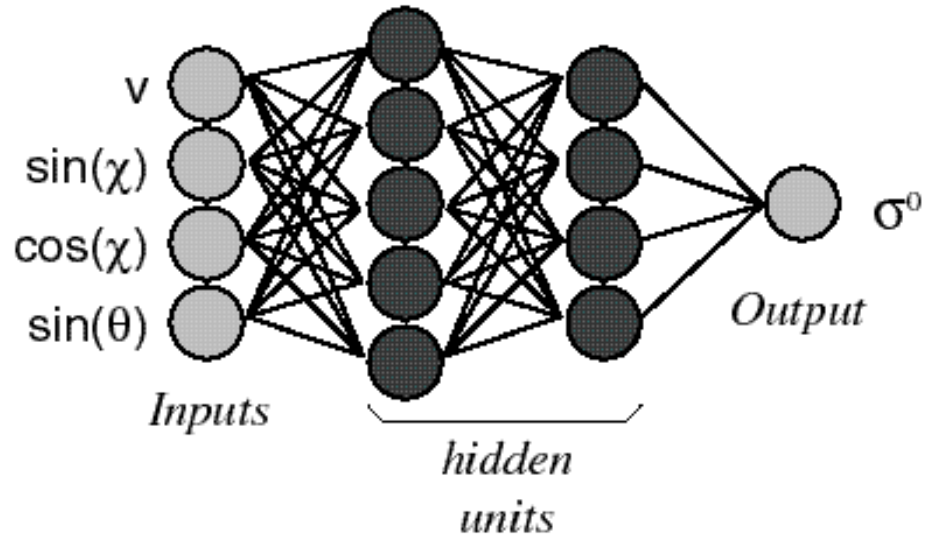


Fig. 2 : Definition of geophysical parameters: the incidence, the azimuth angle.

## Architectures used for the Neural Networks GMF

*For Horizontal Polarization:*



*For Vertical Polarization:*

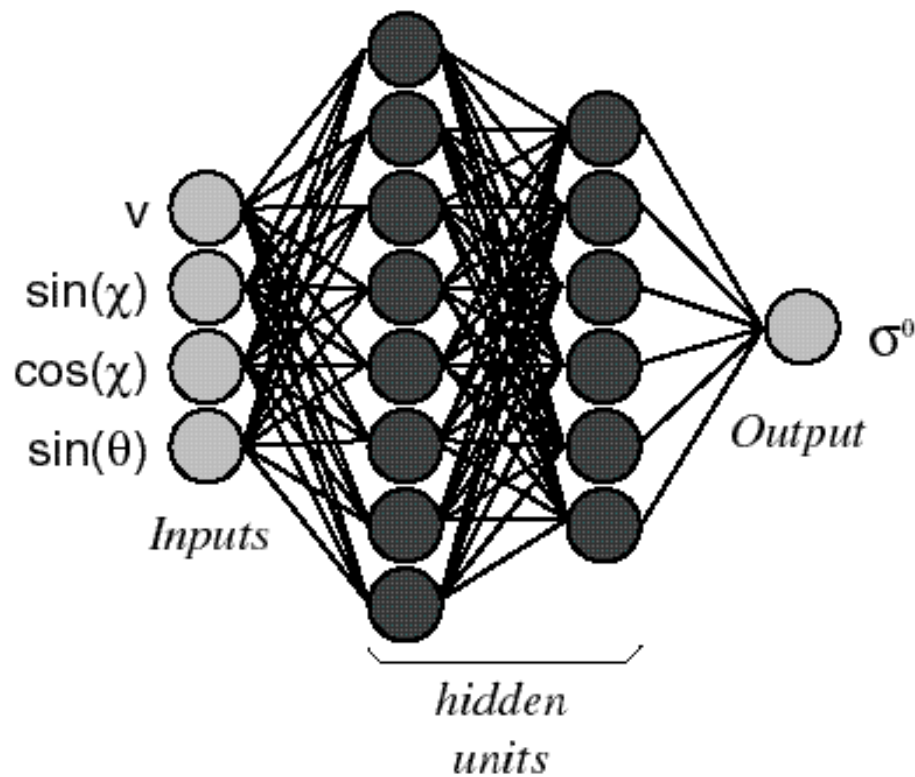


Fig. 3 : Architecture of the neural networks : (a) NN-GMF-H, (b) NN-GMF-V.

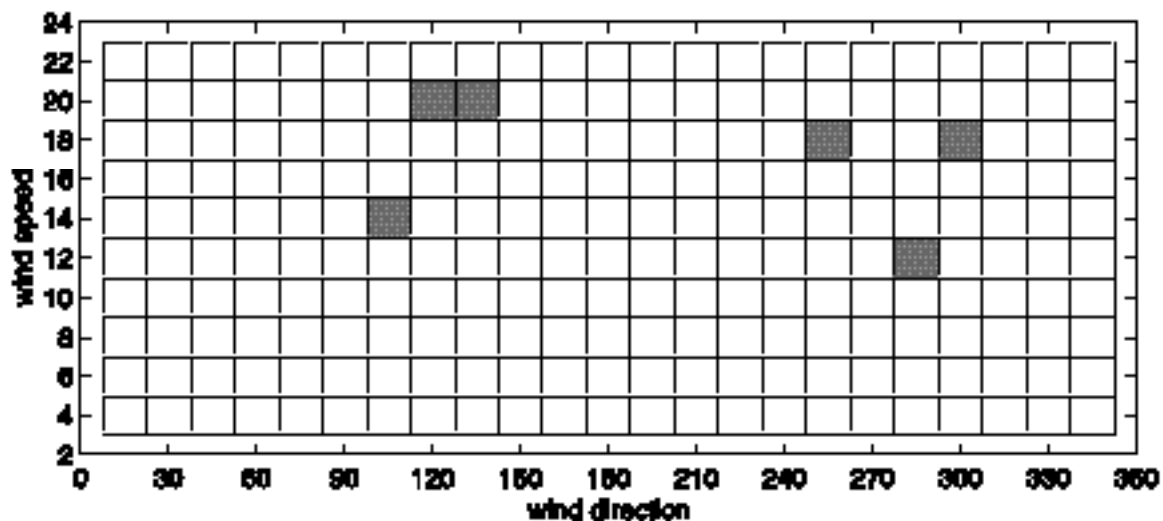


Fig. 4 : Student Test for the NN-GMF-V at an incidence angle of  $36^\circ$  with respect to the wind azimuth and for different wind speeds. When the pixels are white, the test is satisfied with a confidence level of 95% (at a significance level of 5%).

data = CoECMWF MoyTest, Inc = 22.19, N=36554, RMS=1.918, Bias=0.119

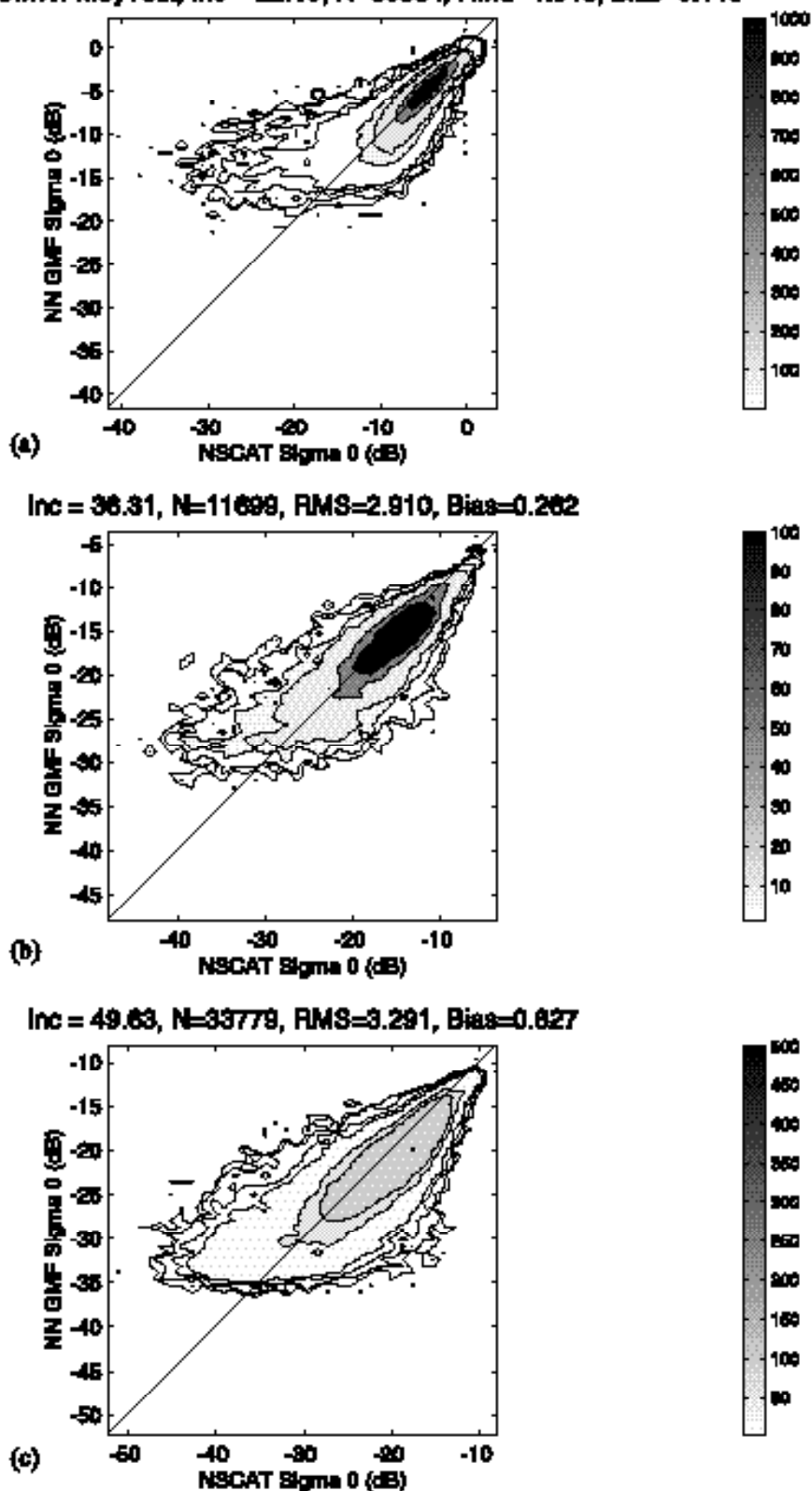


Fig. 5 : Scatter plots of NN-GMF-V versus the NSCAT sigma-0 at three incidence angles : (a)  $=22^\circ$ ; (b)  $=36^\circ$ ; (c)  $=49^\circ$ . The darker the area, the denser the data number. The scale is given in thousands of points.

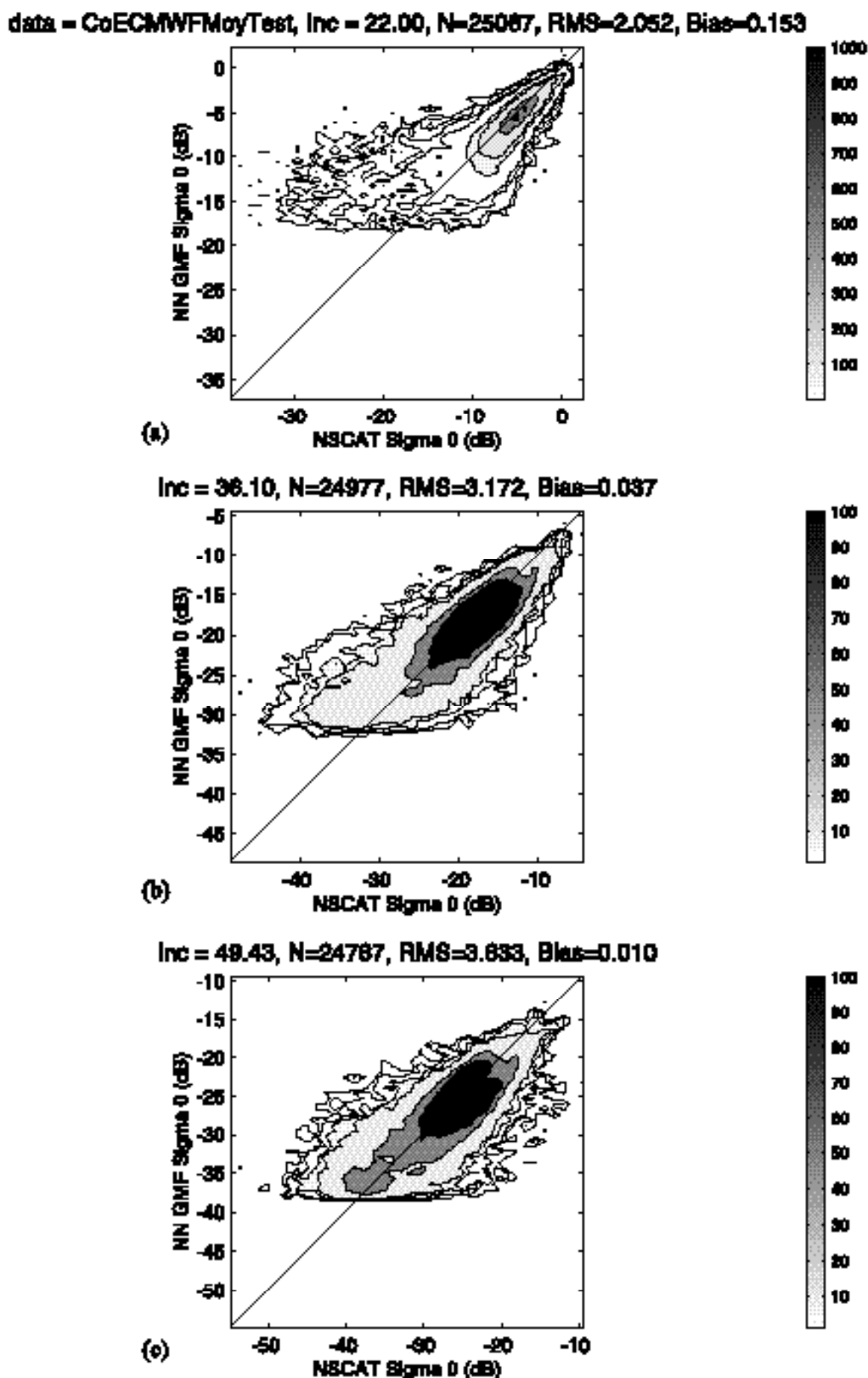


Fig. 6 : Scatter plots of NN-GMF-H versus the NSCAT sigma-0 at three incidence angles. (a)  $=22^\circ$ ; (b)  $=36^\circ$ ; (c)  $=49^\circ$ . The darker the area, the denser the data number. The scale is given in thousands of points.

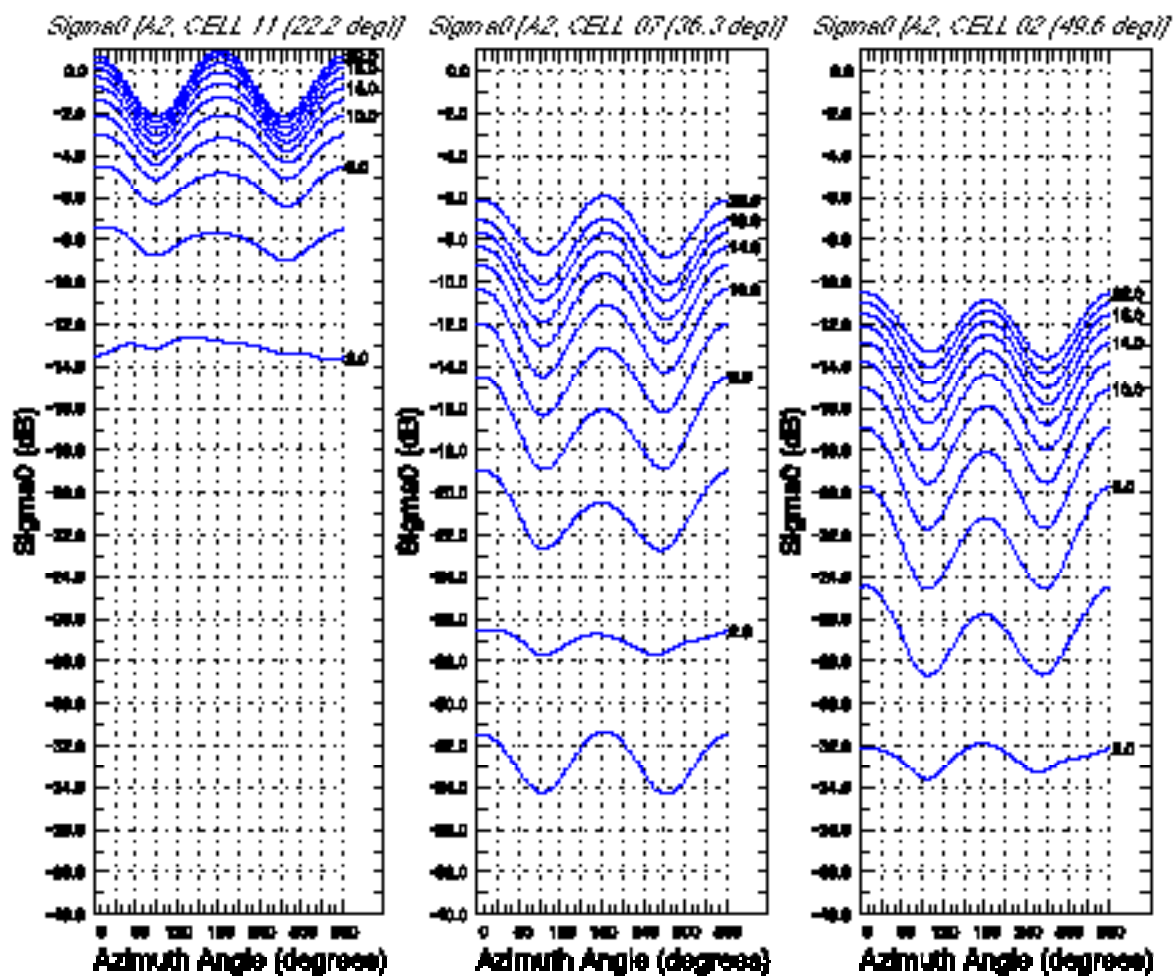


Fig. 7 : Sigma-0 (in dB.) of the NN-GMF-H function with respect to the azimuth angle at different wind speeds at three incidence angles. (a)  $=22^\circ$ ; (b)  $=36^\circ$ ; (c)  $=49.5^\circ$ .

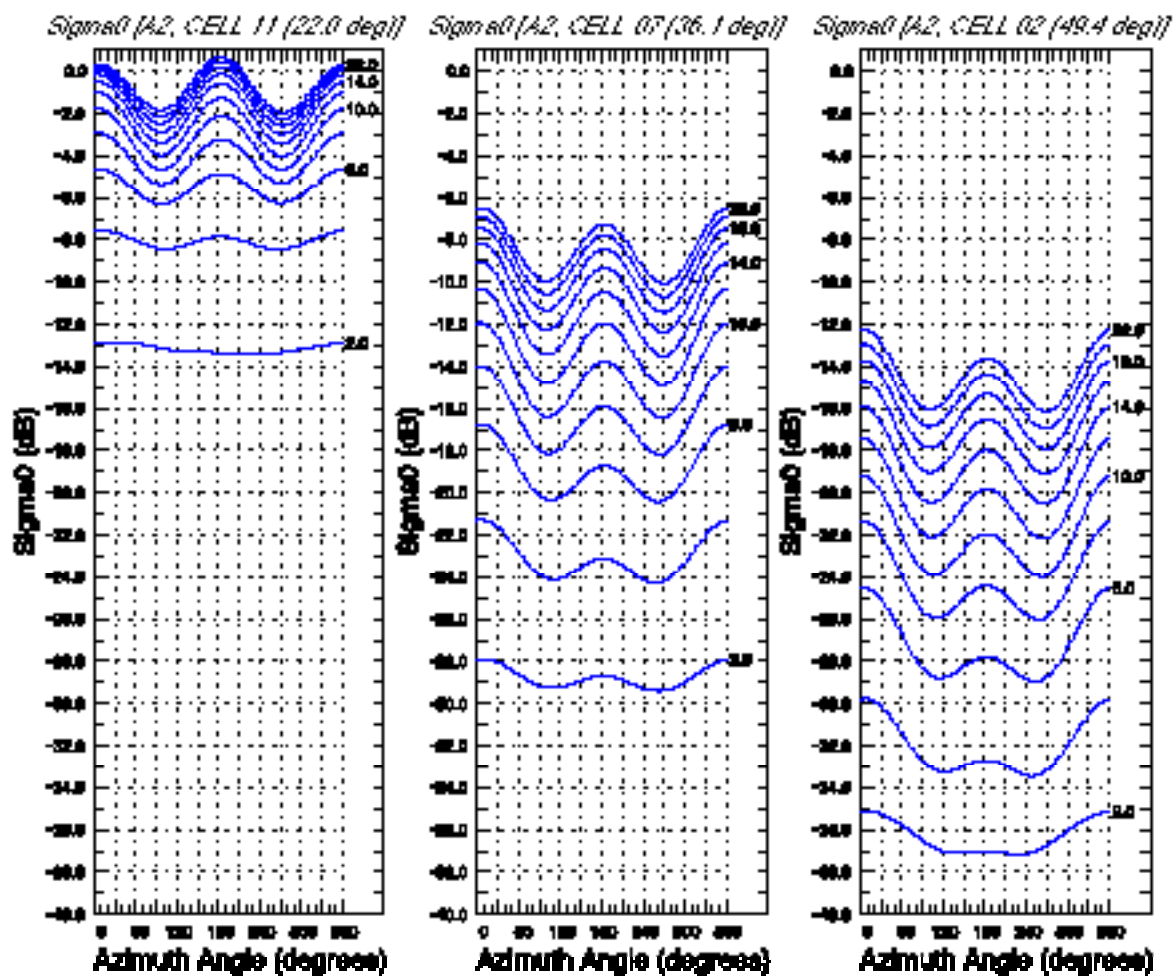


Fig. 8 : Sigma-0 (in dB.) of the NN-GMF-V function with respect to the azimuth angle at different wind speeds at three incidence angles. (a)  $\theta = 22^\circ$ ; (b)  $\theta = 36^\circ$ ; (c)  $\theta = 49^\circ$ ..



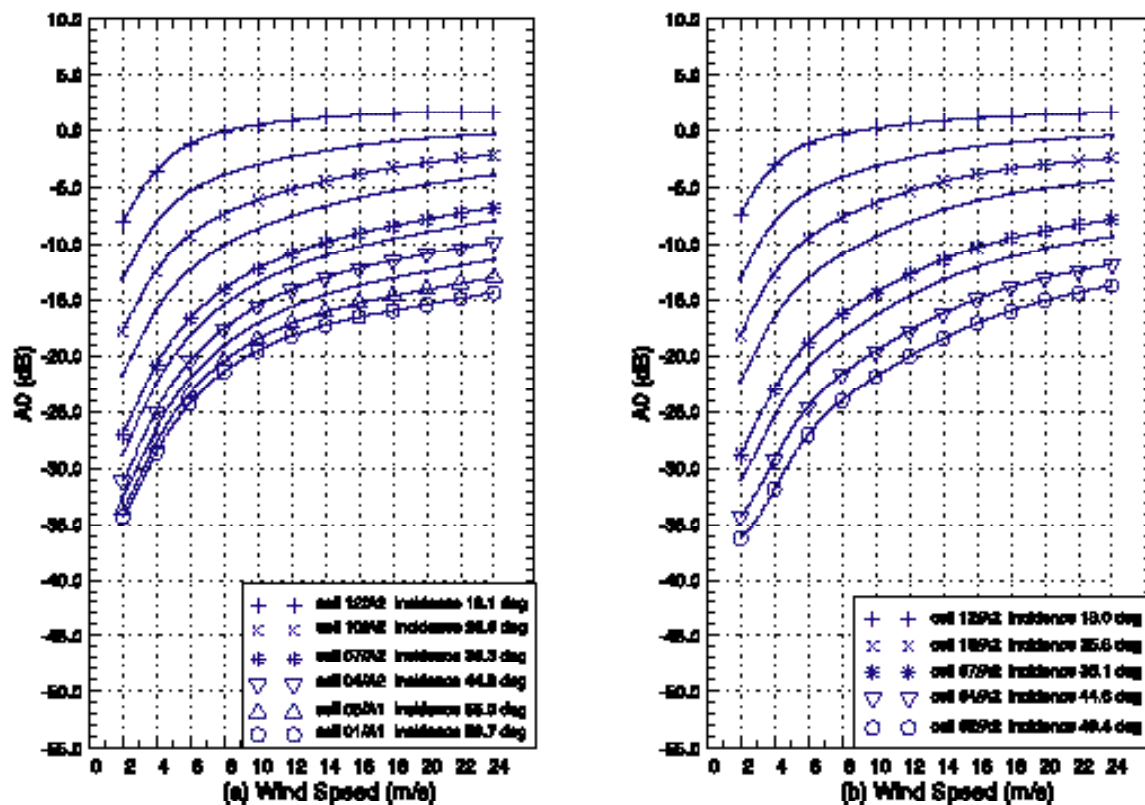


Fig. 9 : Mean values ( $A_0$  Fourier coefficient) of (a) NN-GMF-V and (b) NN-GMF-H versus the wind velocity at different incidence angles. These values are given in dB.

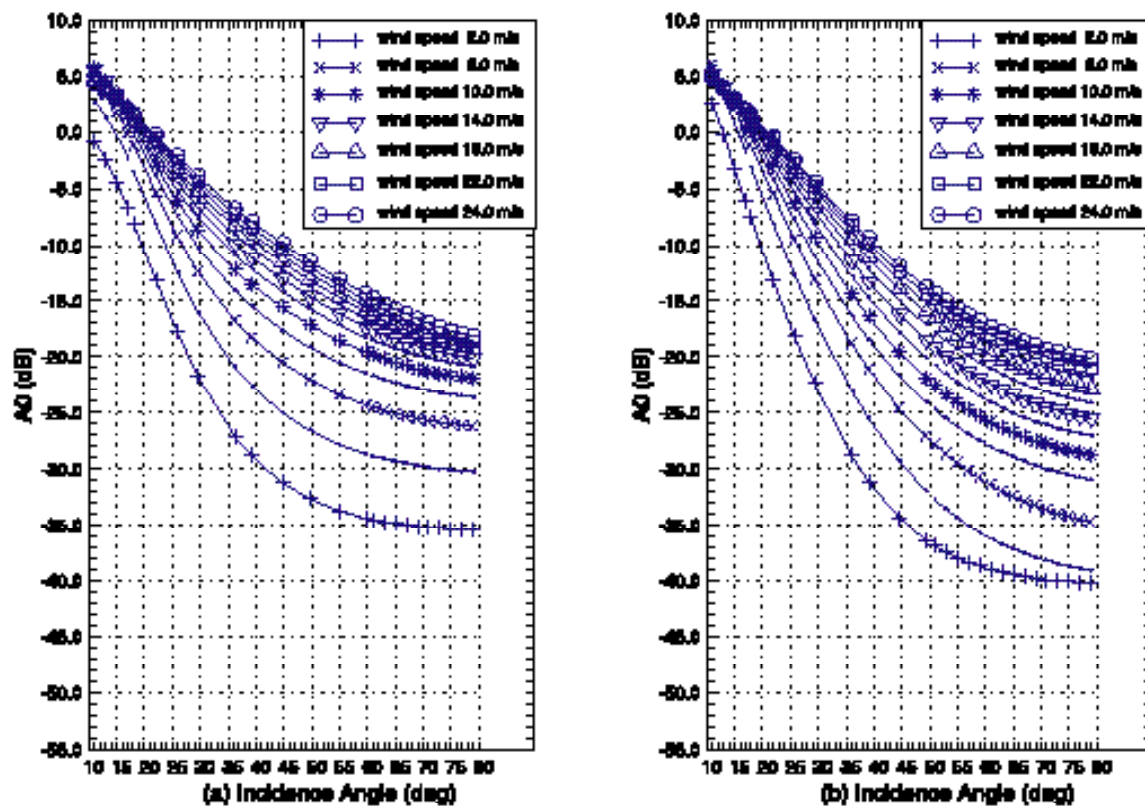


Fig. 10 : Mean values ( $A_0$  Fourier coefficient) of (a) NN-GMF-V and (b) NN-GMF-H versus the incidence angle at different wind velocity. These values are given in dB.

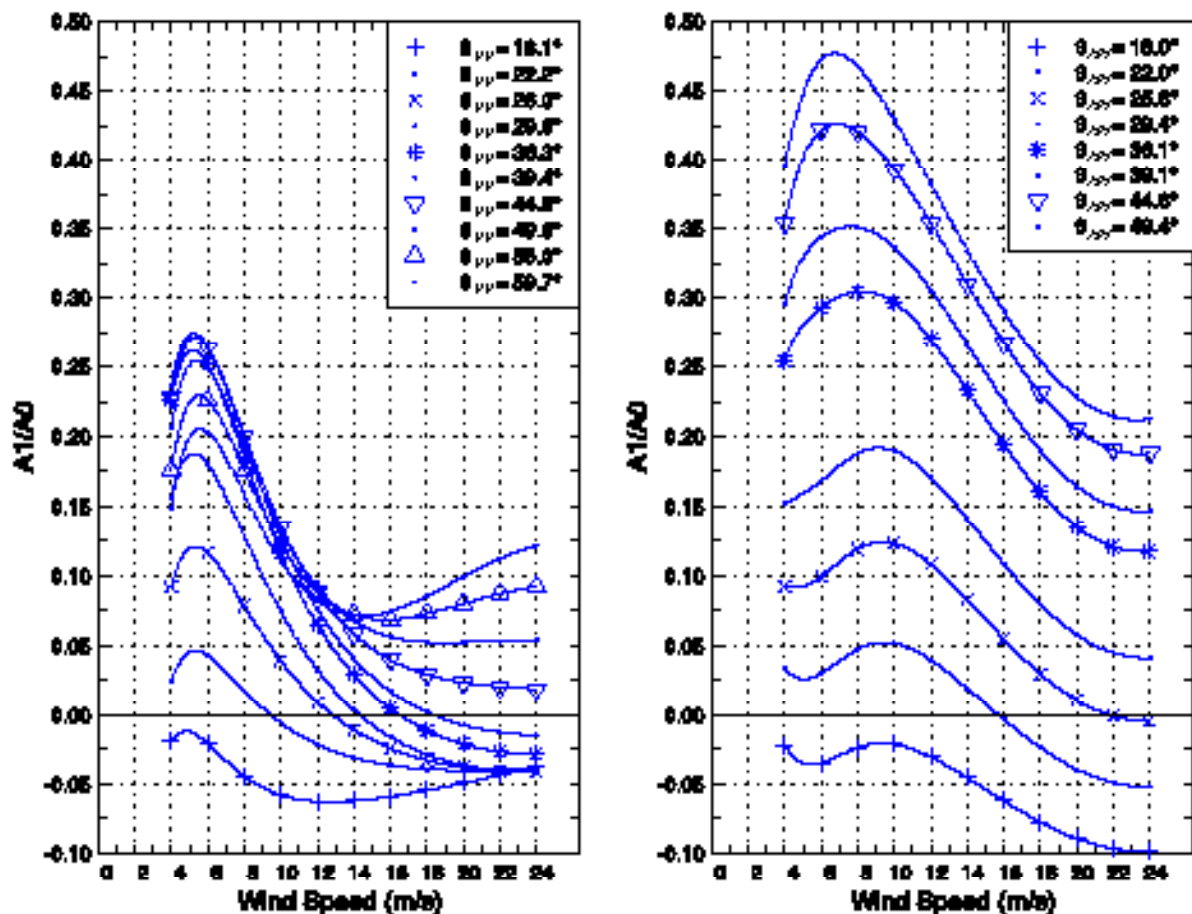


Fig. 11 : Up-wind minus down-wind values ( $A_1$  Fourier coefficient) of (a) NN-GMF-V and (b) NN-GMF-H versus wind velocity at different incidence angles. All these values are given in linear scale.

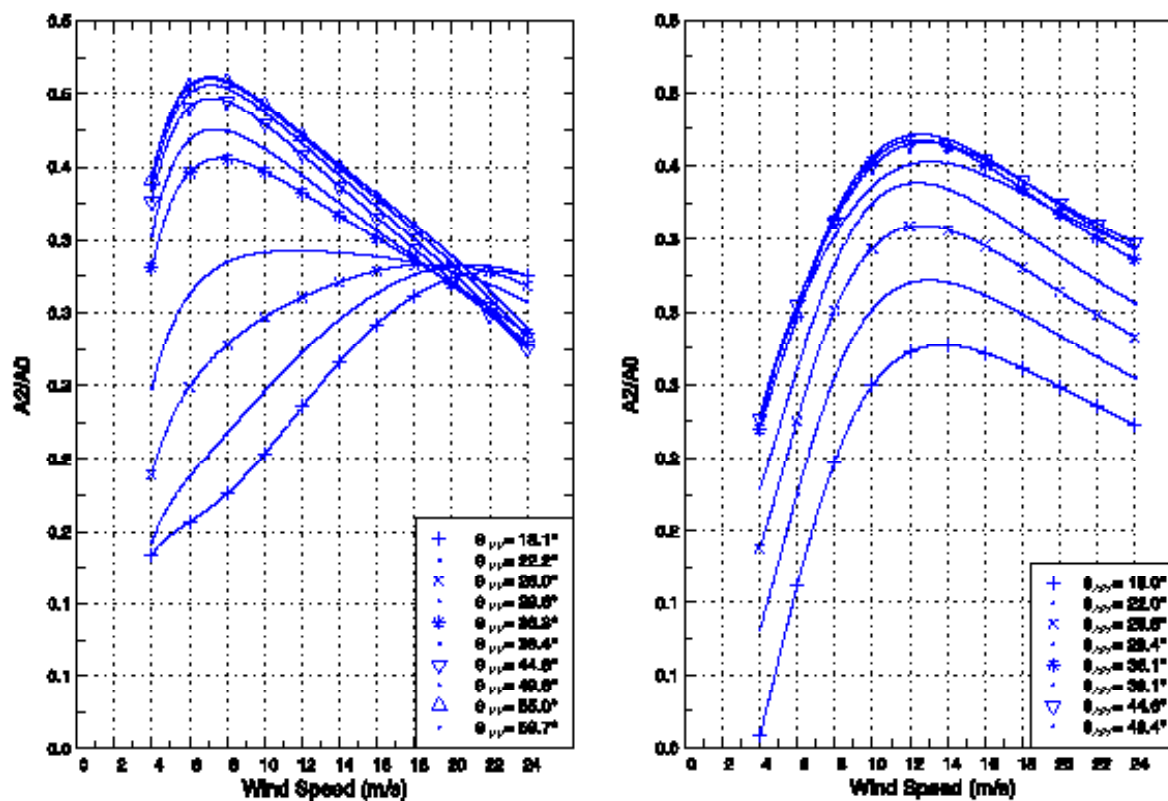


Fig. 12 : Up-wind minus cross wind values ( $A_2$  Fourier coefficient) of (a) NN-GMF-V and (b) NN-GMF-H versus wind velocity at different incidence angles. All these values are given in linear scale.

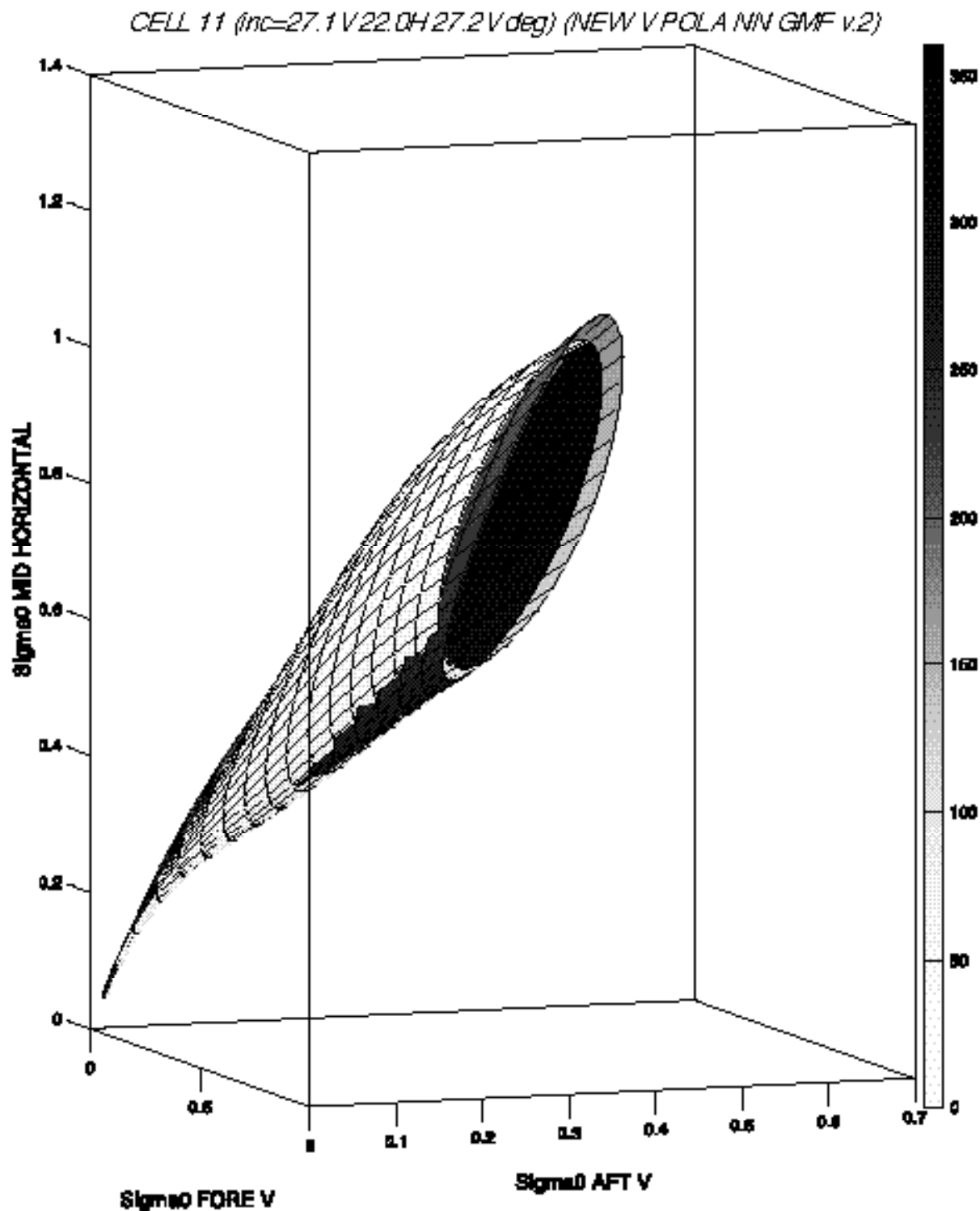


Fig. 13 : Three-dimensional view of a NN-GMF surface corresponding to wind vector solution in the sigma-0 space ( $\sigma_1$ ,  $\sigma_2$ ,  $\sigma_3$ ), where  $\sigma_1$  and  $\sigma_3$  correspond to the vertical polarization at an incidence angle of  $27^\circ$  (fore and aft beams respectively) and  $\sigma_2$  to the horizontal polarization at an incidence angle of  $22^\circ$  (mid beam).

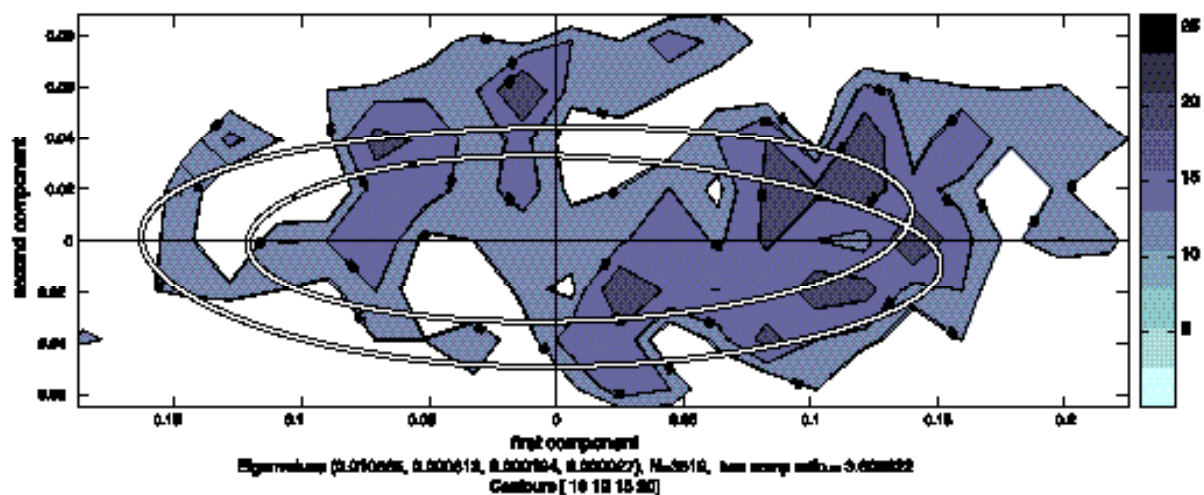


Fig 14 : Simplified projection of the NSCAT cone in the V.V.H. V space against the data corresponding to a wind speed of  $8 \text{ ms}^{-1}$  and incidence angles of  $27^\circ$ ,  $22^\circ$ ,  $22^\circ$  and  $27^\circ$ . The darker the shade, the denser the measurements. The scale is given in thousands of points.

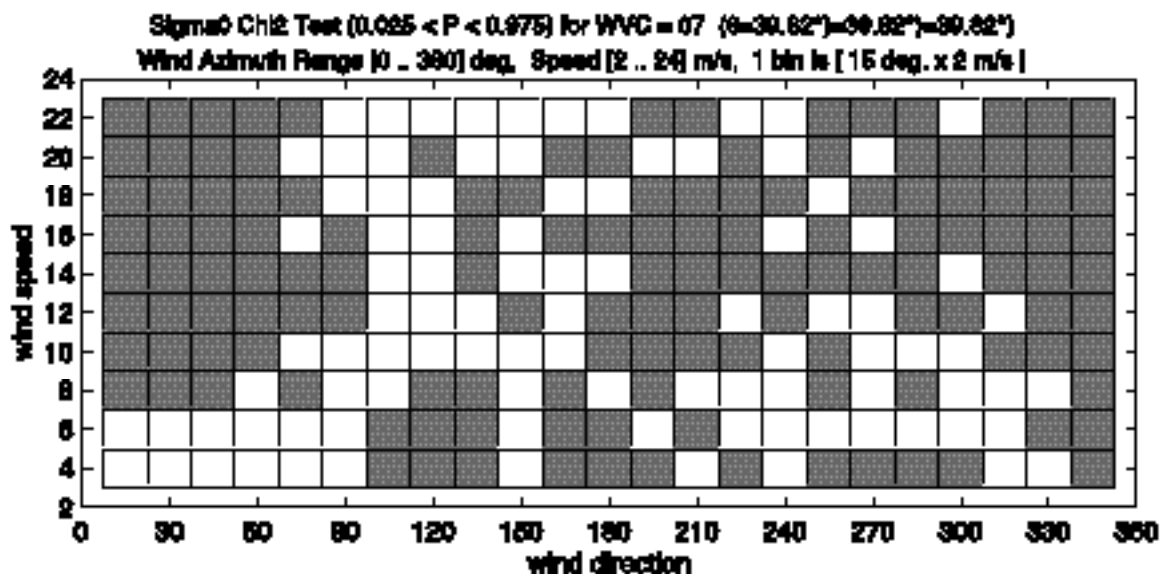


Fig. 15: Chi-2 Test for the NN-GMF-V at an incidence angle of  $36^\circ$  with respect to the wind azimuth and for different wind speeds. When the pixels are white, the test is satisfied with a confidence level of 95% (at a significance level of 5%).

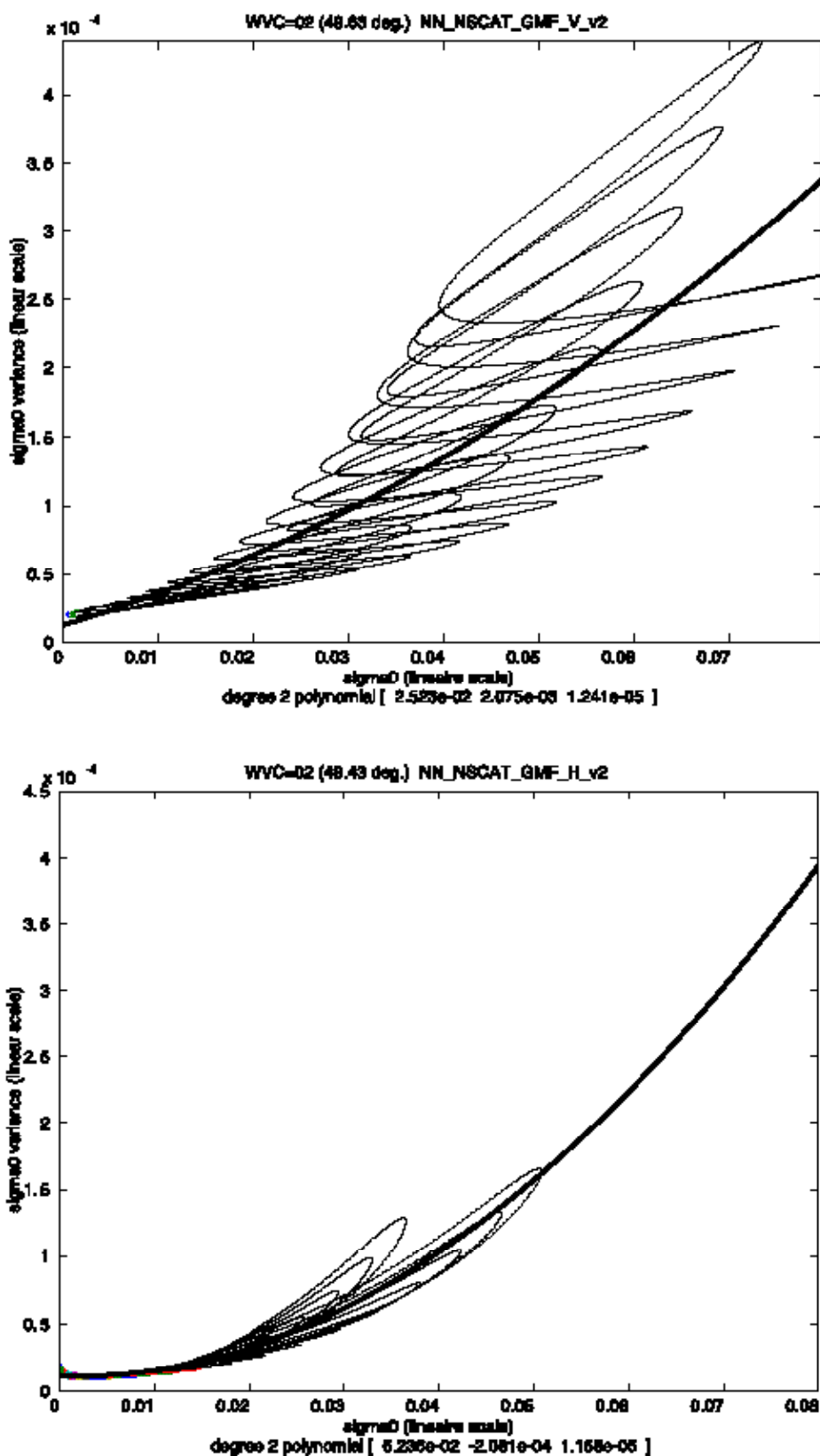


Fig. 16: (a) NN-VAR-V against NN-GMF-V, (b) NN-VAR-H against NN-GMF-H with respect to the wind speed at an incidence of  $49^\circ$ . The trend of the graph (heavy black line) of the NN-VAR relationship is quadratic and of the form of equation (3). The curly pattern of the curve (light line) is a function of the wind azimuth for different speed.



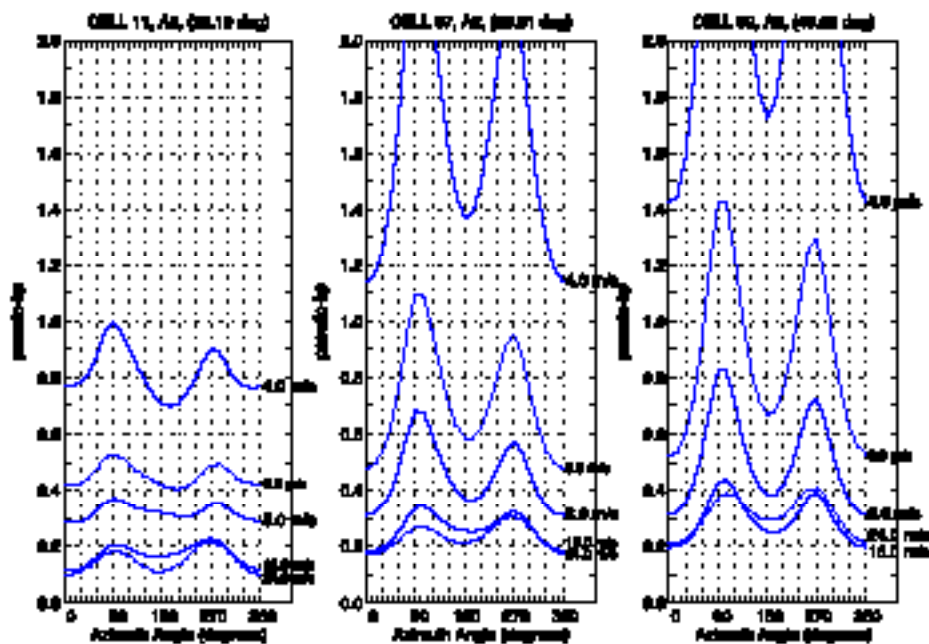


Fig 17 : Signal to noise ratio (so called Kp) corresponding to NN-GMF-V at three different incidence angles ( $22^\circ$ ,  $36^\circ$ ,  $49^\circ$ ) with respect to the azimuth angle and at different wind speeds.

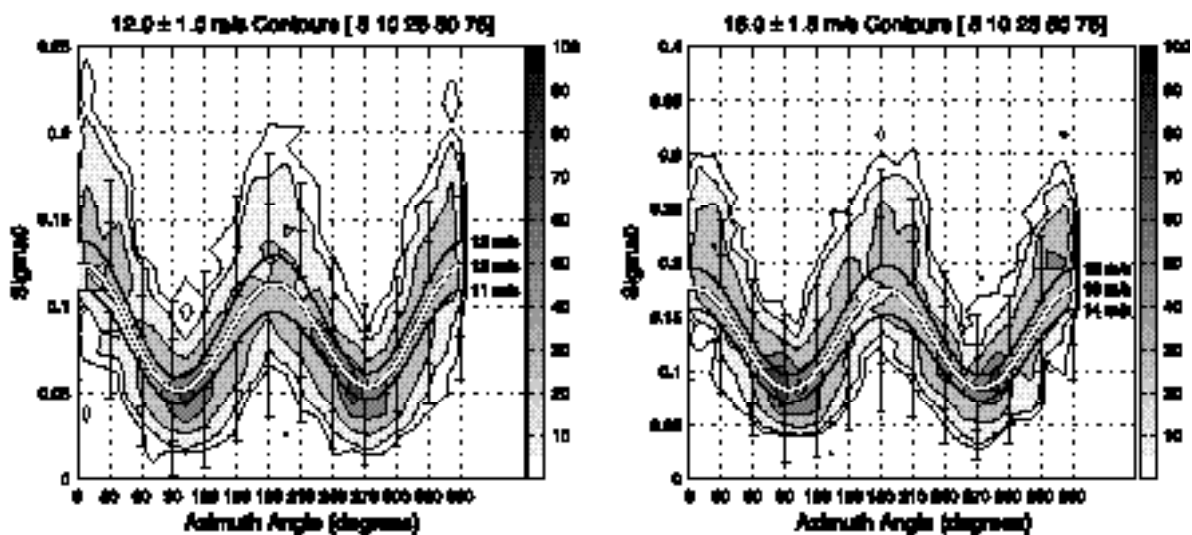


Fig 18 :NN-GMF-V values for different wind speeds (white and black curve) with respect to the azimuth angle for wind speed ranges of  $12\text{ms}^{-1} \pm 1\text{ms}^{-1}$  and  $14\text{ms}^{-1} \pm 2\text{ms}^{-1}$  at an incidence angle of  $36.1^\circ$  against the NSCAT data. In the same figure we plot bars corresponding to one and two standard deviation for some azimuth angles, the standard deviation being derived from NN-VAR results. The darker the shade, the denser the measurements. The scale is given in thousands of points.